DOI: 10.13009/EUCASS2017-227

Flow visualization of the priming process in spacecraft feedlines

C. Bombardieri⋆*, T. Traudt, M. Oschwald*
Engine Transients Group, Institute of Space Propulsion
German Aerospace Center (DLR), 74239 Hardthausen, Germany
⋆Corresponding author: cristiano.bombardieri@dlr.de

Abstract

The start-up sequence of the propulsion system of a satellite or spacecraft involves the opening of the tank isolation valve in order to fill the downstream feedline until the closed thruster valve. This filling process, called priming, can cause severe pressure peaks that could lead to structural failure or even to adiabatic compression detonation in the case of monopropellants such as hydrazine. For safety reasons the feedline is evacuated prior the launch. This causes the propellant to undergo flash boiling, generating a vapor front that mixes with the residual inert gas in the line, usually helium. This complex two-phase/two components flow is quite challenging to model due to a lack of understanding of the physical processes taking place. Therefore an experimental campaign has been conducted at DLR Lampoldshausen in a dedicated test facility which allows fluid transient experiments in the same conditions as the operating space system. Tests are performed at different conditions (tank pressure, vacuum level, geometry of the feedline. . .) with water and ethanol, the latter being the best replacement fluid for the toxic hydrazine in terms of physical properties. In order to gain detailed insight into the complex flow pattern, a quartz segment is installed at the end of the feedline and high speed imaging is performed. The analysis of the images provides a qualitatively comparison between deareated and saturated conditions of the fluid, allowing to explain the complex profile of the pressure signal. In addition, a comparison between water and ethanol shows that the differences in the flow evolution of these two fluids can be related to their physical properties such as surface tension, density and viscosity. This has important implications when testing with the real propellant is not possible and a replacement fluid must be used.

1. Introduction

In the feedlines of a satellite of spacecraft using toxic propellants such as hydrazine or MMH, three barriers are required for safety reasons. The configuration (Fig. 1) foresees three valves, more precisely a pyrotechnic valve, a latch valve and a thruster valve are installed to protect the personnel against potential leakage during the ground operation. In addition the propellant feedlines are usually evacuated prior to launch. Once in orbit, the start-up of the propulsion system of the satellite involves the opening of the pyrotechnic valve, causing the propellant to flow into the evacuated feedline and slam against the closed latch valve. This filling process, called priming, can cause severe pressure peaks that could lead to structural failure. The pressure peak can be estimated by the classical Joukowsky equation for water hammer:

$$P = \rho c V \tag{1}$$

where V is the impact velocity of the liquid front against the closed valve or in general at a dead-end.
In the case of monopropellants such as hydrazine also the risk of adiabatic compression detonation must be taken into account in the design of the feedline subsystem. The works of Briles et al. [1] and Bunker et al. [2] are among the first studies to investigate the detonation hazard of hydrazine. The target of their works was to assess the conditions at which hydrazine undergoes adiabatic detonation.
To prevent undesired high pressure peak, the solution is to slow down the flow through the use of a flow restriction device (venturi [3, 4] or orifice [5]) or by using the gas cushion effect of a pre-filled inert gas in the line. Gibec and Maisonneuve [6] performed priming experiments with real propellants, namely MMH, NTO and hydrazine, for

DOI: 10.13009/EUCASS2017-227

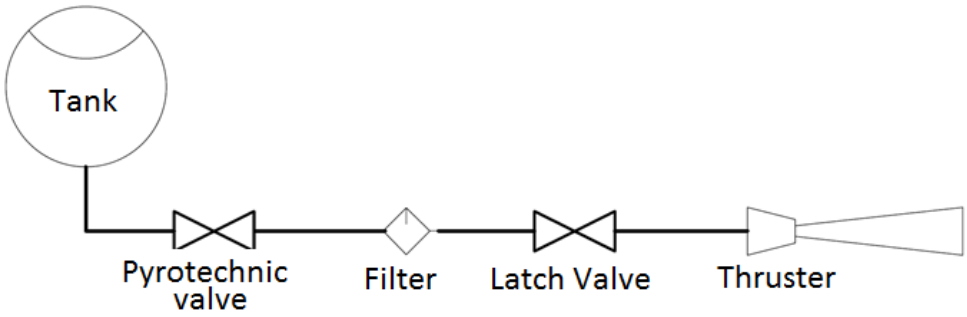

Figure 1: Simplified schematic of a monopropellant propulsion system

different pipe geometries including straight, bend, elbow and tee pipes. They hypothesized that phenomena such as cavitation, pipe deformation and vapor pressure may interfere with the water hammer. Lecourt and Steelant [7] performed several test with ethanol, acetaldehyde and MMH for straight and bend pipes. They observed a surprising multiple steps evolution of the first pressure peak and provided a possible explanation. They also demonstrated that ethanol can be used as a replacement fluid instead of toxic MMH. In his doctoral work, Lema [8] experimentally showed that for a saturated liquid the pressure peak is lower than the deareated case. Due to the gas desorption, the pressure peak also occurs slightly later and the wave damps out faster thanks to the larger volume of released gas.
This paper presents flow visualization obtained with a high speed camera of the priming process in an evacuated pipe. Tests are run with water and ethanol in deareated and saturated conditions. The aim is in particular to explain the peculiar flow pattern observed in previous work of the authors [9].

2. Experimental set-up

2.1 Test Bench description

In order to investigate fluid transient phenomena such as priming and water hammer a dedicated test facility has been built at DLR Lampoldshausen. The Fluid Transient Test Facility (FTTF) reproduces the geometry of the feedline system of a satellite or spacecraft and allows to test at the same real operating conditions. Schematic of the test facility in the priming configuration is shown in Fig. 2. The test bench features a 80 liters run tank pressurized up to 50 bar, a flexible pressurization system (GN2 or GHe as a pressurizing gas) as well as a modular test section with its own conditioning system. Conditioning of the test section can be either done via evacuation or pressurization. The test bench is equipped with a fast opening valve (FOV), pneumatically actuated, mounted on a rigid support to limit vibrations during the opening. Its opening time is only 6 ms and therefore comparable to the one of the pyrotechnic valves (3-5 ms) used in spacecrafts. A valuable feature of the valve is the possibility of purging the valve seat via a purge line. This is of utmost importance to ensure that no gas is present in the valve or in the upstream line after the conditioning of the test-section.

Table 1: Dimensions of the test-bench

Description	
upstream pipe tank-FOV	1023 mm
position of T-branch (MV-2) from tank	550 mm
branch lenght to MV-2	130 mm
FOV seat	16 mm
test-section length	2000 mm
test-section outer diameter x wall thickness	19.05x1.25mm

The geometry of the test-element is a 2000 mm straight stainless steel pipe (1.4541) with a relative large outer diameter (3/4 inch or 19.05 mm) in order to examine high mass flow that are typical of spacecraft feedlines like the ESA

DOI: 10.13009/EUCASS2017-227

Automatic Transfer Vehicle ATV and European Service Module (ESM) of Orion. The wall thickness of the test section is 1.25 mm (ID 16.56mm). At five points the test-section is mounted onto a rigid support structure to limit its movements. The upstream segment, from the tank to the valve, is a OD 22x1.5 mm straight stainless steel pipe with a tee piece inserted 550 mm downstream the tank to allow purging and evacuation. The geometry of the test-bench is summarized in Table 1.
When different configurations are to be tested, the test-element is removed and replaced by the desired geometry. The effect of different set-ups (straight pipes, tees and elbow) on the pressure wave has been investigated by the authors in previous work [9].

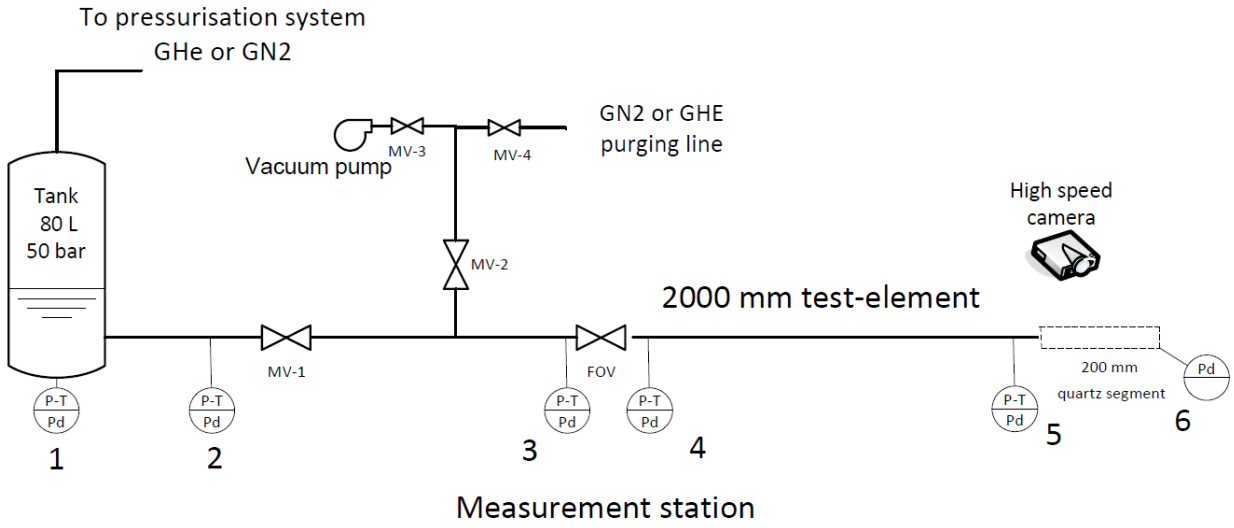

Figure 2: Schematics of M3.5 Fluid Transient Test Facility at DLR Lampoldshausen

In the experiments presented in this paper, the results obtained with the elbow geometry (L) are also included in order to provide an explanation to an open question left unanswered [9]. The elbow set-up is a 1000 mm straight pipe followed by another 1000 mm straight pipe at 90 degree.

Sensors

Measurements of pressure and temperature are performed at different stations as shown in Fig. 2. Each measurement station consists of 3 transducers: one thermocouple type K, 1 kHz sampling rate; one absolute piezoresistive pressure sensor type 4043A200 from *Kistler*, 10 kHz sampling rate; one dynamic piezoelectric pressure sensor type 601A from *Kistler*, 150 kHz sampling rate. To avoid aliasing and high-frequency noise, the filter of the dynamic pressure sensors has been set to 30 kHz. Sensors are screwed in a 20 mm thick disk with the same inner diameter of the pipe to avoid flow disturbances. Dynamic pressure sensors (5.5 mm diameter) and thermocouples are flush mounted, while the absolute pressure sensors are 2 mm beneath the surface through a 1mm hole. The measurement stations are located as follows:

- pos. 1 : at the tank
- pos. 2 : 250 mm downstream of the tank
- pos. 3 : 318 mm upstream of the FOV
- pos. 4 : 160 mm downstream of the FOV
- pos. 5 : 1990 mm downstream of the FOV (10 mm from the dead-end)
- pos. 6 : at the dead-end (only dynamic pressure)

In this work, only the pressure signal of the sensor at the dead-end is used for the analysis. The dynamic pressure sensor at the dead-end is flush mounted to face the fluid, parallel to the center line of the pipe. It is screwed in a measurement module which is connected to the test-section by a Swagelok weld-on fitting.

DOI: 10.13009/EUCASS2017-227

High Speed Camera

A Photron Fastcam SA-X is used for image acquisition. The following settings are used for the video images presented in this paper:

- Frame rate: 19,200 fps
- Resolution: 1024x184

The optical segment is a quartz pipe, 200 mm long and with an inner and outer diameter of 16.56 mm and 31 mm respectively. It is installed at the end of the test section as showed in Figure 3. The overall length of the test-section is therefore 2200 mm.

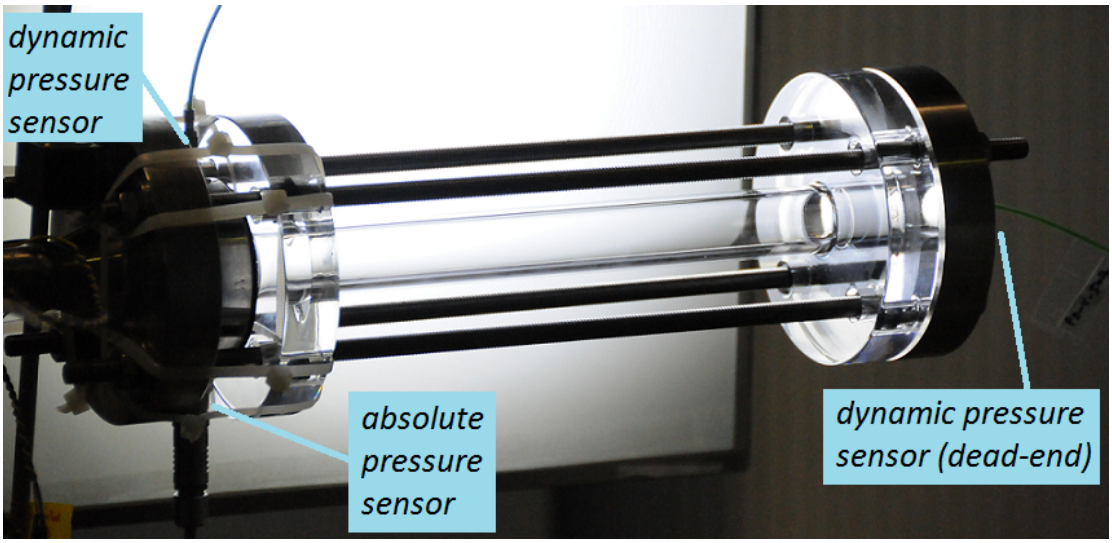

Figure 3: Quartz pipe installed at the dead-end of the test section

2.2 Test Procedure

Before each test the downstream test-section is purged with a gaseous nitrogen (GN2) flow by opening MV-4 and MV-2 (see Figure 1) and unscrewing the measurement module at the test-element end. After this operation, the test-section is evacuated by means of a vacuum pump (MV-3 open). The fast opening valve (FOV) and MV-2 are then closed and MV-1 is opened to manually prime the upstream pipe. At this point, automatic operations are performed by the controlling software: the tank pressure is set at a given value, the trigger command for data acquisition is given (-500 ms), as well as the trigger for the high speed camera, and FOV opens (time: 0 ms). Data are recorded for 4 seconds.

2.3 Test-matrix

The aim of the test campaign is to perform visual investigations of the flow pattern during priming with water and ethanol. The pressure in the test element (P_{line}) is kept at near vacuum, while the tank pressure varies according to the fluid used. The tank pressure in the real operating systems is usually 20 bar, however, for safety reason, lower tank pressures are set in the present tests, as listed in Table 2.

Table 2: Test-matrix: tank pressure for the flow visualization with the quartz pipe

Geometry	Tank pressurizing condition	water P_{line} : 10 mbar	ethanol P_{line} : 20 mbar
straight pipe (2200 mm)	deareated vs saturated	9 bar	5.5 bar
elbow (1000 mm + 1200 mm)	deareated vs saturated	7 bar	7 bar

DOI: 10.13009/EUCASS2017-227

The tested geometries are the straight pipe and the elbow (L). Both fluids are investigated in deareated and saturated conditions. For the latter, gaseous nitrogen is used as a pressurizing gas. Tests are repeated three times for each test condition to examine reproducibility.

3. Test Results

When the saturated liquid is primed into the evacuated line, it will not only undergo flash evaporation, but it will also release the dissolved pressurizing gas (desorption) at a given rate. The solubility of a gas into a liquid is described by Henry's law, which states that the amount of dissolved gas is proportional to its partial pressure. The proportionality depends on the equilibrium temperature and pressure. The amount of the dissolved GN2 in water and ethanol is listed in Table 3. Values are taken from [10, 11].

Table 3: Solubility of nitrogen in water and ethanol

Nitrogen solubility		
gas saturation pressure	water	ethanol
1 bar	20.8 mg/kg at 293 K	220 mg/kg at 293 K
20 bar	380 mg/kg at 293 K	4200 mg/kg at 298 K

Straight pipe: deareated vs saturated ethanol

High speed imaging allows a qualitatively comparison between deareated and saturated conditions. Some significant images during the initial filling are shown in Fig. 4, including the pressure profile and the corresponding pressure points. These are chosen at the most meaningful pressure levels, such as at the first filling of the segment (1-4), at half point of the rise (6), at the peak (7) and at the valley (8). Deareated fluid is depicted on the left (L) in Fig. 4 while the saturated one on the right (R). Tank pressure is set at 5.5 bar for safety reasons. A first difference is noted in the conditions at which ethanol enters the dead-end: deareated fluid appears as a very tiny mist (1L), while the saturated one arrives instead as a mixture of bubbles and mist (1R). The more coarse pattern of saturated ethanol is visible in the following frames (2-3-4), whereas the deareated one appears not only finer but also more homogeneous. The pressure profile (R) at around 1-4 presents more spikes: this noise-like appearance in the signal is due to the individual bubbles that impact on the sensor pressure. The desorbed GN2 creates gas pockets and enhances the formation of bigger liquid droplets/slugs. This same mechanism can be described for saturated water.
The higher amount of desorbed gas can be seen by comparing frames 6-7-8. The gas bubbles are in fact somewhat bigger, in particular toward the end of the segment at its right. At its left (at the entrance of the quartz pipe) a dark cloud is present in both fluids (7-8): this is the initial residual gas that gets trapped as the main liquid front arrives. At the maximum pressure level (7) this cloud is bigger for the saturated case due again to the added gas coming from the desorption process. The release of the dissolved gas causes the pressure peak to be smaller (21.0 bar vs 24.9 bar), due to the additional damping effect.

Elbow geometry: water vs ethanol

In previous work of the authors [9], an unexplained pressure profile was observed in case of the elbow set-up, with a remarkable difference between water and ethanol. In the case of water and elbow configuration, the first pressure peak shows a double spike, with the first spike at 153 ms and the second spike at 160 ms. This characteristic is also observed in case of deareated water, but is not present in the case of deareated ethanol (Fig. 5). A comparison between deareated and saturated water shows an almost identical pressure profile, with the minor difference that the curve is smoother for the deareated case. This indicates that the release of the dissolved gas introduces high frequency effects related to the gas bubble dynamics making the pressure signal look more noisy. The reason of the double spike is possibly related to two different slugs of liquid impinging at the dead-end. The first slug detaches from the main flow due to the elbow, inducing the first pressure peak of 80 bar; it is then followed by the main flow which generates the actual water hammer pressure peak.
The case of ethanol is more interesting, since it poses various questions. With deareated ethanol, the curve is smooth and regular, as in the straight pipe. When ethanol is saturated instead, the curve exhibits the double spike as similarly

DOI: 10.13009/EUCASS2017-227

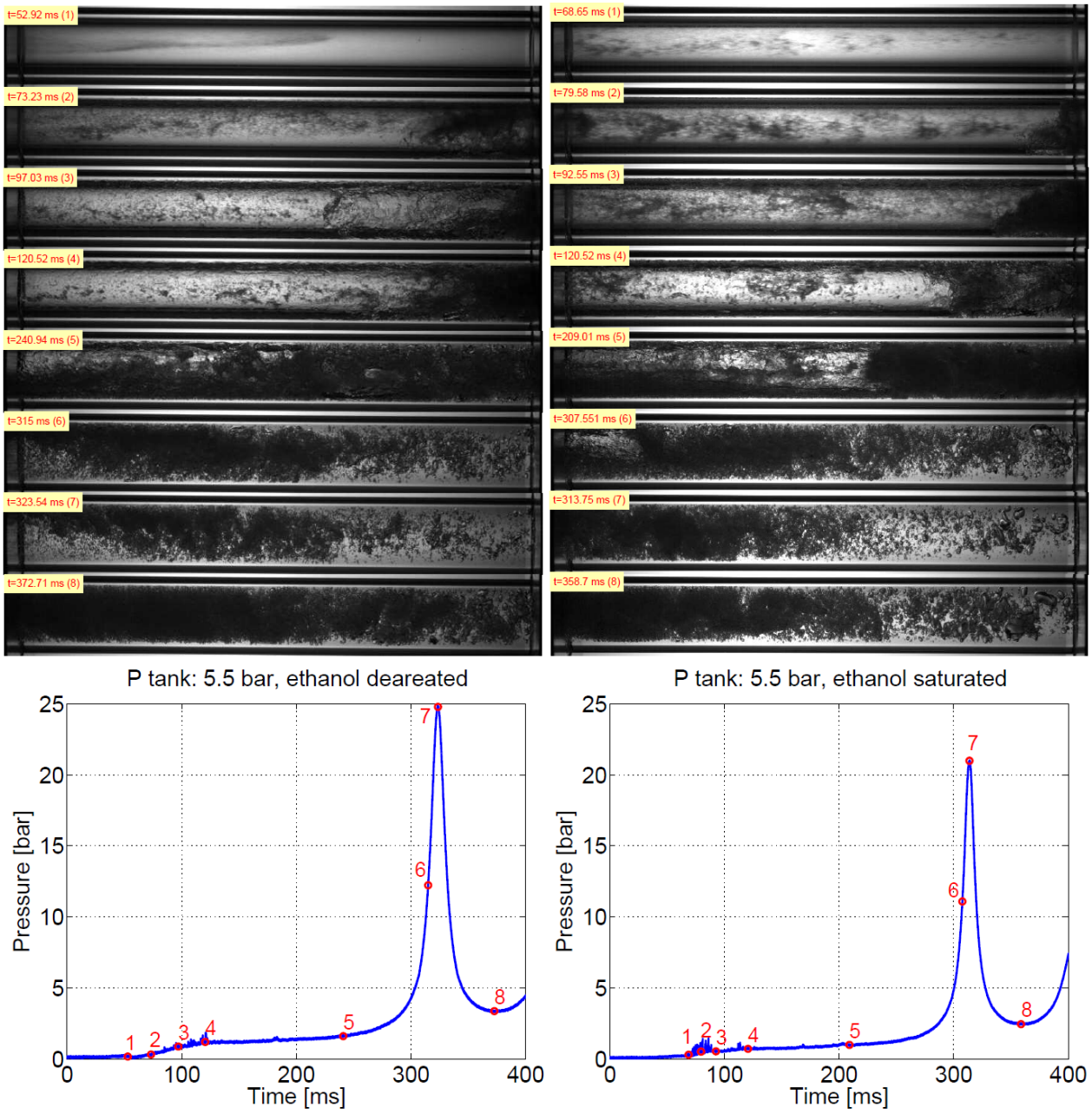

Figure 4: Video frames of the filling of the pipe at the dead-end and corresponding pressure points. Left: deareated ethanol, right: saturated ethanol; line pressure: 20 mbar for both cases

described for water. The pressure loss at the elbow enhances the gas desorption from the liquid and induces the separation of a liquid slug that precedes the main flow and hits the dead-end, as explained for water. The argument against this explanation is why this occurs also for deareated water. Since no gas is released, the only physical fluid properties which might justify the generation of a slug flow regime are the fluid viscosity and the surface tension. The flow pattern of liquid-gas flow in horizontal pipes is widely investigated due to its important industrial applications. Unfortunately, all the proposed flow regime maps hold for stationary flow, with well-defined and constant liquid velocity and gas velocity. These conditions are far from the actual situation occurring during priming, where the fast transients and the flash boiling dominate the physics. As a general rule the flow regime depends mainly on the phase velocities[1] rather than fluid properties. Keeping this limitations in mind, some general remarks might nevertheless be of help in understanding the difference between ethanol and water. The effects of fluid properties on the two-phase flow pattern

[1]The use of phase velocity allows to define Reynolds number and to introduce the Kelvin-Helmotz instability as the main mechanics for regime transition.

DOI: 10.13009/EUCASS2017-227

transition was investigated by Weisman et al. [12]. The transition from stratified flow to wave flow depends on the parameter $\sigma^{0.2}/\mu^{0.45}$, with higher values to shift toward slug regime. Ethanol has smaller surface tension than water (22 vs 72 mN/m) and higher viscosity (1.40 vs 1.14 mPa·s), thus this will hindered the transition towards wave flow, which precedes the slug regime.
Sadatomi et al. [13] investigated the effect of the surface tension on the gas-liquid flow in horizontal pipe, observing that the fluid with a lower surface tension generates smaller bubbles which easily coalesce and promote the transition from bubbly flow to slug flow. This is in contrast with the actual test results. Andritsos et al. [14] focus instead on the effect on viscosity, concluding that a fluid with higher viscosity will hinder the initiation of slug flow. That is in line with the test results, and would allow to affirm that the viscosity is more important than the surface tension, at least in the formation of this particular pressure profile.
A more classical approach based on the Reynolds number can also provide a plausible explanation. As known, in classical fluid dynamics the Reynolds number is often used to define flow patterns and flow transitions. The flow velocity is not know, but it can be approximated by $V \approx \sqrt{P_{tank}/\rho}$, neglecting the friction losses. Therefore the Reynold number is

$$Re = \frac{\rho V D}{\mu} = \frac{\sqrt{\rho}\sqrt{P_{tank}}D}{\mu}$$

The actual Re is not calculated, nor it would be of some use in these fast transient conditions. What could be of help is the ratio between the Re of water and the Re of ethanol:

$$\frac{Re_{water}}{Re_{ethanol}} = \frac{(\sqrt{\rho}/\mu)_{water}}{(\sqrt{\rho}/\mu)_{ethanol}} = 1.4$$

In the same conditions, water has a 40% higher Reynolds number. This means that the transition to slug pattern is easier for water than for ethanol.

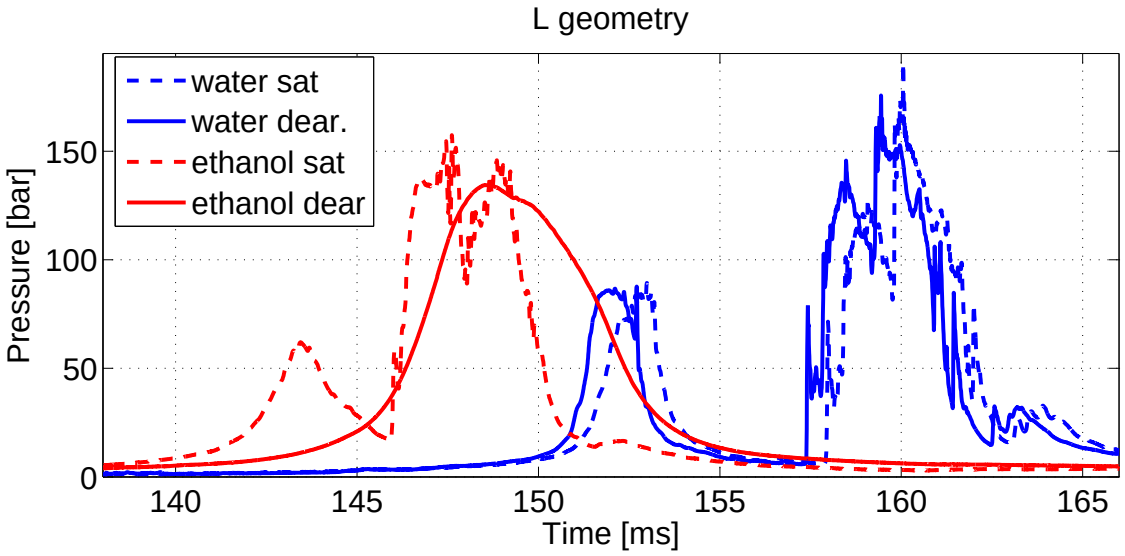

Figure 5: Comparison between deareated and saturated conditions in the L geometry

This has important implications in case a replacement fluid is to be used for testing instead of a toxic propellant, such as the case of ethanol considered as the best replacement for MMH [7]. Therefore, in selecting a replacement fluid, the surface tension, the viscosity and the density are the fluid key-properties which shall be as similar as possible to the original propellant in order to ensure that the physical behavior is reproduced.

High Speed Imaging of priming in elbow

Some significant snapshots during the priming in the L geometry for deareated water are shown in Fig. 6, while the corresponding pressure points and the general pressure profile are plotted in Fig. 7. Tank pressure is 7 bar. Frame (1) is shown to allow comparison with (2), where the image gets blurry (it can be clearly seen at the dead-end, where the gasket is not visible anymore). This indicates that vapor arrives at the dead-end after 88 ms and it condenses on

DOI: 10.13009/EUCASS2017-227

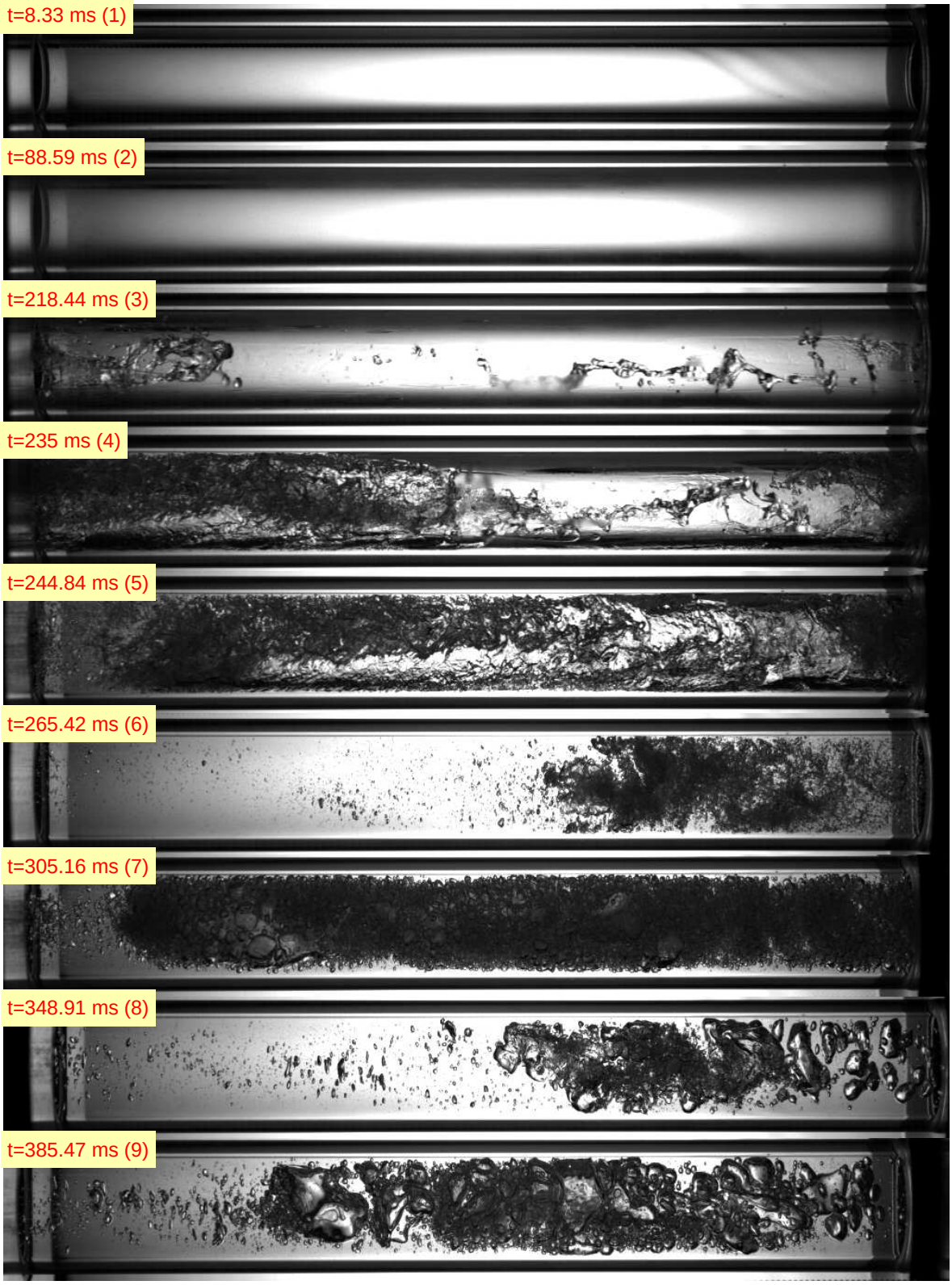

Figure 6: Video frames of the filling at the dead-end for the L configuration. Fluid is deareated water; tank pressure: 7 bar; line pressure: 10 mbar

DOI: 10.13009/EUCASS2017-227

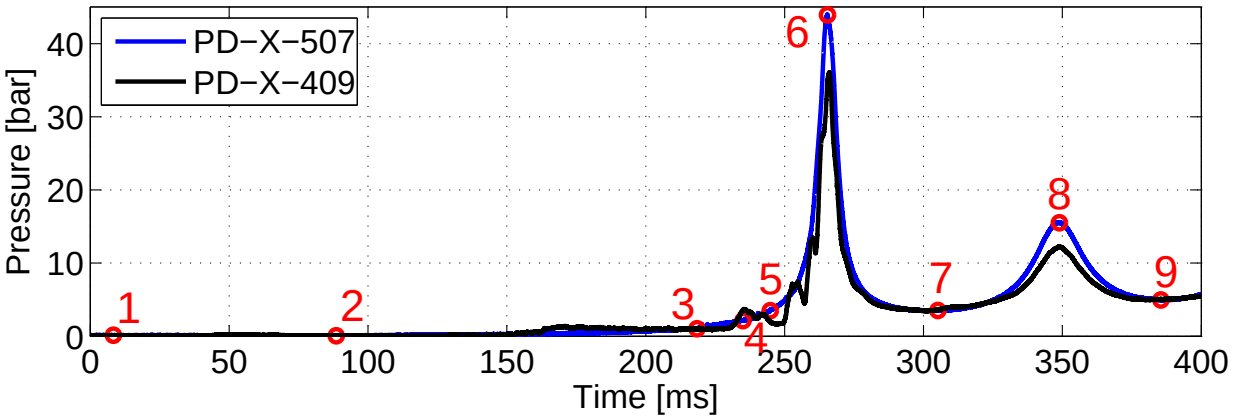

Figure 7: Pressure profile and the corresponding points of the selected snapshots. Sensor PD-X-507 is at the dead-end, while PD-X-409 is at the elbow

the colder wall. The vapor front travels well ahead of the liquid and is remarkably fast considering that the first liquid droplets arrive after 218 ms (3). As known by the classic fluid dynamics, a pipe elbow creates a swirling secondary flow, which can be identified in (4): unlike the case of straight pipe where the flow is stratified in top/bottom direction, now the liquid wets the front side of the pipe. At 244 ms (5) the main liquid front enters the optical segment and causes a sudden increase in the pressure, visible in the pressure curve of the sensors at the elbow (PD-X-409). The pressure profile at the elbow recalls the double spike characteristic observed previously at the dead-end. At 20 bar driving pressure, the secondary flow will impact at higher velocity and also with higher mass flow, generating the first pressure spike that is not visible with the present 7 bar tank pressure. Frame (6) and (8) captures the flow pattern at the two first pressure peaks: the minor pressure at (8) makes the gas bubble considerable bigger than in (6). It is also interesting to note the remarkable displacement of the pipe itself during this fast transient. Comparing (8) and (9), the branch moves of about 4 mm; in fact the elbow configuration is known to induce the strongest pipe displacements during fast fluid transients.

4. Conclusions

At the dedicated Fluid Transient Test Facility of DLR Lampoldshausen, flow visualizations of the priming process in evacuated pipelines have been performed with water and ethanol. The aim of the test campaign is to gain insight into the flow evolution, in particular to qualitatively assess the difference between deareated and saturated condition of the fluid. The analysis of the images has shown that the released gaseous nitrogen, dissolved during the storage in the tank, creates gas pockets and enhances the formation of bigger liquid droplets/slugs, affecting therefore the evolution of the flow pattern. The desorbed gas also accounts for the additional damping of the pressure peak with respect to the deareated case.

The elbow geometry causes not only a reduction of the pressure peak with respect to the straight pipe, but also a different shape in the pressure profile. This is intimately connected to the fluid conditions and to the fluid properties: major difference exist between deareated and saturated ethanol, while no remarkable differences are observed between deareated and saturated water. A detailed explanation based on the fluid properties has been proposed. The authors speculated that the surface tension, the density and the viscosity are the fluid key-quantities responsible for the two-phase flow pattern transition. This has important implications when testing with the real propellant is not possible and a replacement fluid must be selected in order to ensure that the physical behavior is correctly reproduced.

Further flow visualizations will be performed by installing the quartz pipe in different locations along the test-section, such as downstream the main valve and at the elbow, in order to be able to characterize the flow regime in the whole pipe.

Acknowledgments

The authors wish to thank the M3/FTTF technicians for their support in the test preparation.

DOI: 10.13009/EUCASS2017-227

References

[1] O. Briles and R. Hollenbaugh. Adiabatic compression testing of hydrazine. In *AIAA/SAE 14th Joint Propulsion Conference*, Las Vegas, 1978.

[2] D.L. Bunker, R.L.and Baker and Lee J.H.S. Explosive decomposition of hydrazine by rapid compression of a gas volume. *Dynamics of Detonations and Explosions: Detonations. Progress in Astronautics and Aeronautics*, pages 325–341, 1991.

[3] Henry C Hearn. Development and application of a priming surge analysis methodology. In *41st AIAA/ASME/SAE/ASEE Joint Propulsion Conference & Exhibit*, 2005.

[4] A.R. Scroggins. A streamlined approach to venturi sizing. In *48th AIAA/ASME/SAE/ASEE Joint Propulsion Conference & Exhibit*, volume 2012-4028, 2012.

[5] Michael J. Morgan. Pressure transient characterization test for star-2 propulsion system fuel manifold. In *40th AIAA/ASME/SAE/ASEE Joint Propulsion Conference and Exhibit*, 2004.

[6] I. Gibek and Y. Maisonneuve. Water hammer tests with real propellants. *AIAA*, 4081, 2005.

[7] Renaud Lecourt and Johan Steelant. Experimental investigation of waterhammer in simplified feed lines of satellite propulsion systems. *Journal of Propulsion and Power*, 23:1214–1224, 2007.

[8] M. Lema. *Multiphase Fluid Hammer: Modeling, Experiments and Simulations*. PhD thesis, Universite' Libre de Bruxelles, 2014.

[9] C. Bombardieri, T. Traudt, and C. Manfletti. Experimental study of water hammer pressure surge in spacecraft feedlines. *6th European Conference for AeroSpace Sciences (Eucass), Krakow*, 2015.

[10] Kai Fischer and Michael Wilken. Experimental determination of oxygen and nitrogen solubility in organic solvents up to 10 mpa at temperatures between 298 k and 398 k. *The Journal of Chemical Thermodynamics*, 33(10):1285 – 1308, 2001.

[11] Junji Tokunaga. Solubilities of oxygen, nitrogen, and carbon dioxide in aqueous alcohol solutions. *Journal of Chemical & Engineering Data*, 20(1):41–46, 1975.

[12] J. Weisman, D. Duncan, J. Gibson, and T. Crawford. Effects of fluid properties and pipe diameter on two-phase flow patterns in horizontal lines. *International Journal of Multiphase Flow*, 5(6):437 – 462, 1979.

[13] M. Sadatomi, A. Kawahara, M. Matsuo, and K. Ishimura. Effects of surface tension on two-phase gas-liquid flows in horizontal small diameter pipes. *Journal of Power and Energy Systems*, 4:290–300, 2010.

[14] N. Andritsos, L. Williams, and T.J. Hanratty. Effect of liquid viscosity on the stratified-slug transition in horizontal pipe flow. *International Journal of Multiphase Flow*, 15(6):877 – 892, 1989.